# Density Functional Study of the Reaction of Carbon Surface Oxides: The Behavior of Ketones

**Karina Sendt* and Brian S. Haynes**

*Department of Chemical Engineering, University of Sydney, New South Wales 2006, Australia*

*Received: October 26, 2004*

The reactions of a ketone surface oxide group have been studied on two forms of the zigzag edge and the armchair edge of a model char using density functional theory at the B3LYP/6-31G(*d*) level of theory. Rearrangement and surface migration reactions were found to occur much more rapidly than desorption reactions on both the zigzag and armchair edges. A number of desorption pathways characterized here go some way toward explaining the experimentally observed broad activation energy profile for CO desorption. Three separate desorption processes were characterized; on the zigzag surface two were found with activation energies of 275 and 367 kJ mol$^{-1}$, while on the armchair surface one was found with an activation energy of 296 kJ mol$^{-1}$. The activation energies for these processes were found to be insensitive to increasing the size of the char fragment. On a larger char fragment, however, an extra desorption process was found to be possible, with an activation energy of 160 kJ mol$^{-1}$.

## 1. Introduction

An understanding of the oxidation of carbon and the role of carbon surface oxides in this process has been the subject of many studies over the years due, originally, to the importance of this process in energy-producing combustion systems and, more recently, to the emerging area of carbon materials and nanotubes.

Experimentally, a range of surface oxides has been identified, and the oxidation rates of different carbons vary widely. To account for the diverse behavior of a range of carbonaceous materials, it has long been held that the reactions of surface oxides must be understood and modeled correctly.

Recently, a turnover model has been developed,[1] which successfully describes the observed reaction behavior of a model carbon. This model describes a population of surface oxide complexes undergoing formation, reaction, and decomposition and is based on the stochastic variable $E_{des}$, the activation energy required for desorption of the oxide. The desorption behavior of carbon oxides has been studied using temperature-programmed desorption (TPD)[2] and shows a broad activation energy profile ranging from 150 to over 400 kJ mol$^{-1}$, with a peak at 300 kJ mol$^{-1}$. It is not clear whether this broad profile is a consequence of a range of surface oxides, a range of carbon structures, or both. Although the turnover model provides a good kinetic description for the gasification of carbon, it provides no mechanistic understanding of the underlying processes taking place on the carbon surface. Applying quantum chemical methods to identify important pathways and surface intermediates is a promising approach to understanding carbon gasification reactions.

Computational quantum chemical techniques have been applied to describe the properties and energetics of oxides on model graphite chars. A recent review by Zhu et al.[3] summarizes much of the work in the area, in particular the work by Yang and co-workers that investigates the interaction of $O_2$, $CO_2$, and $H_2O$ with the zigzag surface of graphite.[4,5] They propose that the rate of gasification of surface oxides is enhanced by the presence of $O_2$ which binds to the surface in an out-of-plane configuration, but they have not provided any kinetic evidence for this.

Montoya and co-workers have also studied the interaction of $O_2$, $CO_2$, $H_2O$, and CO with the zigzag and armchair surfaces of model graphite structures[6−8] and were the first to compute a rate constant for a carbon gasification reaction.[9] They found that the gasification of CO from a ketone on the zigzag surface proceeded according to the expression $k(T) = 1.81 \times 10^{17} \exp[-47682/T(\mathrm{K})]$ ($s^{-1}$), equivalent to an activation energy of 396 kJ mol$^{-1}$. More recently, Frankcombe and Smith[10] disputed their findings, suggesting that loss of CO from the zigzag surface occurred via two pathways: a direct reaction, with activation energy of 166 (singlet) and 401 kJ mol$^{-1}$ (triplet) or via a surface intermediate, with activation energy of 149 (singlet) and 121 kJ mol$^{-1}$ (triplet).

This study will concentrate on desorption, rearrangement, and surface migration reactions of a ketone group on both the zigzag and armchair surfaces of a model char. A ketone group is conceivably one of the simplest oxides on the carbon surface, with a single oxygen atom bound to a vacant carbon site, without any rearrangement of the underlying carbon structure. Ketone functional groups have been observed experimentally and could be formed through a number of reaction processes: chemisorption of $O_2$ on an edge site followed by surface migration until the two oxygen atoms are well-separated; adsorption of $O_2$ on the basal plane followed by $O_2$ bond cleavage and surface diffusion to a vacant site; or deposition of an oxygen atom on the surface by a molecule such as $CO_2$.[4]

Although the desorption of CO from a zigzag surface has been studied previously as described above, there is obviously disagreement as to the mechanism and kinetic behavior for the gasification of CO from the zigzag surface. Additionally, there has been no study of possible surface migration reactions to adjacent vacant sites on the zigzag surface or any kinetic study of the behavior of ketones on the armchair surface. Both

* Corresponding author. E-mail: ksendt@chem.eng.usyd.edu.au.

10.1021/jp045111p CCC: $30.25 © 2005 American Chemical Society
Published on Web 03/26/2005

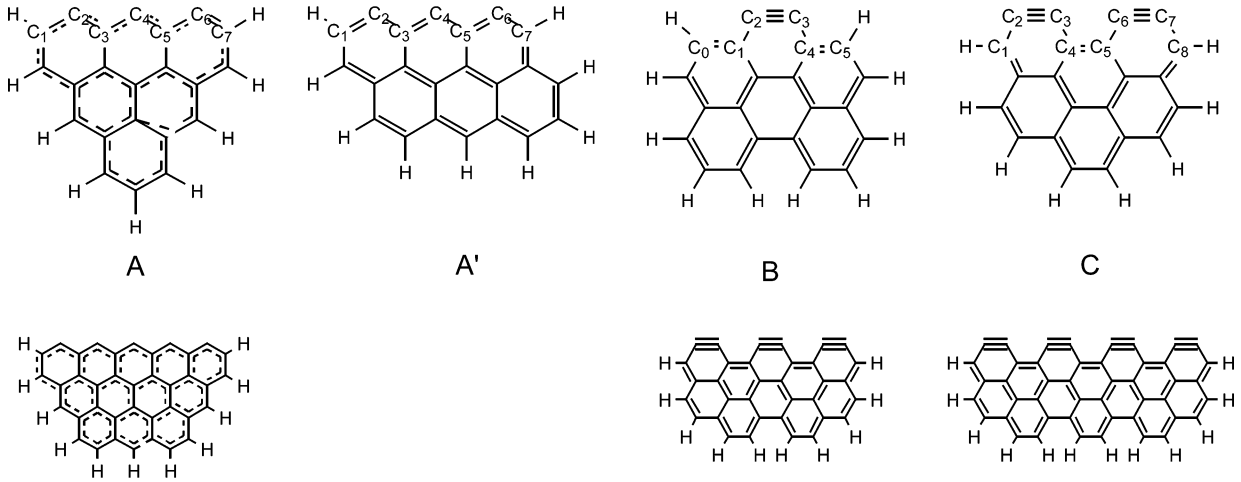


**Figure 1.** Model char molecules: A = non-Kekulé zigzag edge; A′ = Kekulé zigzag edge; B and C = armchair edges. Top row represents basic six-ring model chars; bottom row represents extended or large model chars.

rearrangement and surface migration reactions for other oxides have been shown to be competitive to desorption reactions on the armchair surface.[11]

The aim of this work is to provide a kinetic understanding of the behavior of a ketone on the zigzag and armchair surfaces. This will include resolving confusion surrounding the issue of gasification of CO from the zigzag surface.

## 2. Computational Methods

**Choice of Model Char.** The four model chars used in this work, each with six aromatic rings, are illustrated in Figure 1. The first two of these (A and A′) were used to model the reactions on the zigzag edge, with model A containing three rows of aromatic rings and having $C_{2v}$ symmetry and model A′ containing two rows of aromatic rings and having $C_s$ symmetry. The model char A is derived from a non-Kekulé polynuclear aromatic which has a triplet ground state and is highly symmetric,[12] while model char A′ is derived from the isomeric Kekulé structure. The third model char (B) was used to model decomposition, rearrangement, and some migration reactions on the armchair edge, while the fourth (C) was used to model the remaining migration reaction on the armchair edge. Molecules of this size with edge carbon atoms terminated by hydrogen atoms have been shown to reproduce experimental data for polyaromatics,[13] and predicted molecular properties were found to be relatively size-independent above this minimum size.[13]

The zigzag models (A and A′) in this study were chosen to have six aromatic rings in order that there would be three unpaired electrons with three active sites rather than four unpaired electrons for three active sites as is required for the five-ring models used previously.[9,10] No substantial difference attributable to model size could be found between the six-ring model A used here and the five-ring model used previously.[9,10] Models A and A′, however, have an uneven number of electrons due to the extra ring and doublet and quartet states based on A and A′ correspond to singlet and triplet states respectively in previous work. Because model A has a higher degree of symmetry than model A′, both stable intermediates and transition states were characterized for model A, while stable intermediates were characterized for model A′ in order to understand the effect of varying the underlying char structure.

Lignite and a bituminous coal, prepared by pyrolysis over the temperature range 900−1250 K, were found to have a polynuclear aromatic domain size of the order of 16−24 atoms (4−7 rings), as measured by $^{13}$C NMR spectroscopy.[14] The average number of aromatic rings per plate of carbon micropores was calculated to be 11.6 (standard deviation of 7.9), the equivalent of about 38 carbon atoms by a reverse Monte Carlo simulation.[15] The simulation included only complete six-atom ring structures (no nonaromatic rings or dangling carbons), but it does give an indication of the size of aromatic fragments in real carbons. Larger model chars, as shown in Figure 1, were also used to model equilibrium structures, as there has been some suggestion that five- and six-ring model chars do not accurately represent the graphite limit.[10]

**Choice of Method.** Density functional theory (B3LYP) has been used throughout this work with the 6-31G(*d*) basis set. This has been used successfully to obtain accurate geometries and energies of graphene structures[13] and has been shown to have little spin contamination in these systems.[16] The unrestricted formalism was used for all states; while it is not the best method for very accurate description of low-spin biradical systems, it has been shown to provide a reasonable description of singlet biradicals for molecules of this type.[17] Higher level multireference methods which include electron correlation are not currently computationally feasible for these systems due to their size and the large number of $\pi$ electrons. Geometries, energies, and vibrational frequencies were computed at the B3LYP/6-31G(*d*) level of theory for all stationary points. Several multiplicities for each species were considered, and where electronic states were close in energy, contributions from both electronic states to the electronic partition function were included, with the higher spin-state geometry, energy, and vibrational frequencies used to calculate the remaining partition functions. Geometries were optimized using redundant internal coordinates, which has been shown to be preferable for polycyclic systems.[18] Transition states were identified by the presence of a single imaginary frequency, and the intrinsic reaction coordinate was followed if there was any ambiguity about the nature of the transition state. Transition-state theory was used to calculate high-pressure rate constants in the temperature range of 300−2000 K and fitted to a two-parameter Arrhenius form in this temperature range. Where the calculated barrier of reaction was close in energy to the endothermicity of the reaction, variational transition-state theory was used. In practice, the rate constant was calculated as a function of the breaking bond length (in ∼0.1 Å increments), and the rate

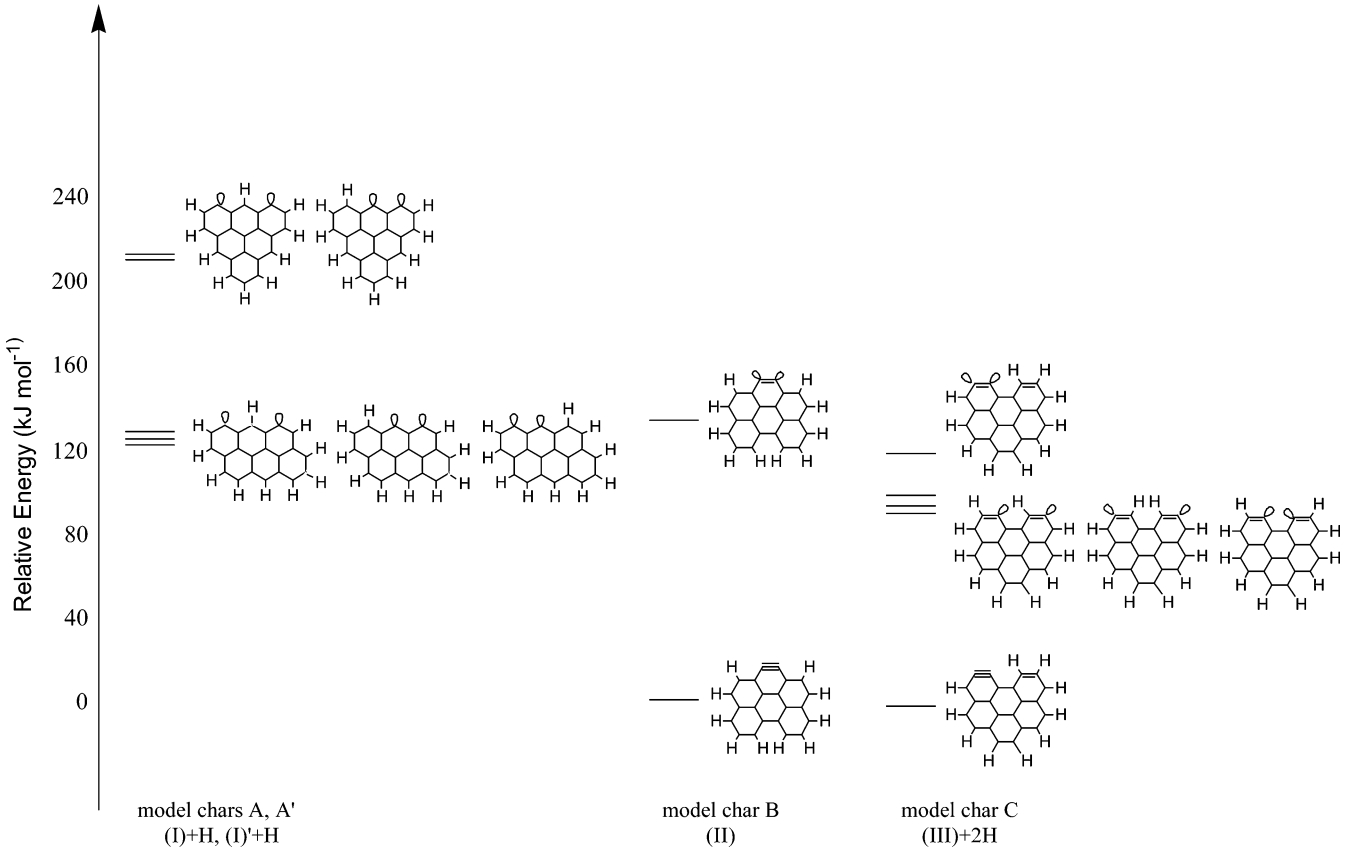


**Figure 2.** Energetics of various $C_{22}H_{10}$ isomers. Comparison of model chars with two vacant sites (one H added to A and A′, 2H added to C).

constant for each temperature was taken to be the minimum. Where intermediates and transition states were found to be slightly nonplanar, they were treated as planar for the purpose of allocating a symmetry number, $\sigma$, and the number of optical isomers, $m$. Most of the nonplanar species fell into this category, and exceptions are discussed further in the text. Due to symmetry in some of the oxide structures, the rate constants reported here sometimes include multiple pathways (e.g. migration both to the left and to the right), and this is discussed when the situation arises. The quantum chemical calculations were carried out using NWChem4.0[19] and Gaussian98.[20]

## 3. Results and Discussion

A comparison of the energetics of the zigzag and armchair surfaces is shown in Figure 2. Selected geometrical parameters for each of the species discussed are presented in Figure 3. Figures 4−9 contain schematics for the potential surfaces for the desorption, rearrangement and migration reactions on the zigzag and armchair surfaces. Relative energies for species included in the kinetic analysis are presented in Tables 1 and 2 for the zigzag and armchair surfaces, respectively. Kinetic parameters calculated for each of the reactions are presented in Table 3.

**Comparison of Zigzag and Armchair Surfaces.** The structure of the zigzag edge has been given some attention in previous work,[21,22] albeit at a much lower level of theory than discussed here. In short, the edge consists of carbon atoms alternating between those which are bound to three other carbon atoms and satisfy the octet rule (odd numbered in this work) and those which are bound to only two carbon atoms and have an unpaired electron (even numbered in this work). The latter are available for edge complex formation, while the former are available more properly for basal plane complex formation.

There are three unpaired electrons in (I) in Figure 2, with a quartet ground state and the (biradical) doublet state 16 kJ mol$^{-1}$ higher in energy. Although remnants of the non-Kekulé singly occupied orbitals can be seen in the wave function of the quartet state of (I), somewhat delocalizing the unpaired electrons around the entire edge of the model char, the three unpaired electrons are predominantly located at $C_2$, $C_4$, and $C_6$. In (I), the bond length along the zigzag edge varies between 1.37 and 1.41 Å. The Kekulé isomer of (I) based on model A′, denoted (I)′, is 86 kJ mol$^{-1}$ more stable, with the three unpaired electrons located simply on $C_2$, $C_4$, and $C_6$. Clearly, the arrangement of aromatic rings can have an effect on the thermodynamic stability of char structures. An allene-type edge exists at considerably higher energy on the doublet surface and has not been considered further in this study.

The structure of the armchair edge has been given less attention in combustion chemistry as it was assumed to be unreactive;[22] however, the carbon nanotube community has characterized the edge.[23] The armchair edge consists of pairs of carbon atoms alternating between those which are bound to three other atoms (numbered $C_0$, $C_1$, $C_4$, $C_5$, ... in this work) and those bound to two other atoms (numbered $C_2$, $C_3$, $C_6$, $C_7$, ... in this work). All the atoms on the edge satisfy the octet rule, with those bound to only two atoms forming a triple bond, giving a benzyne-like structure to the edge. The ground state of the armchair edge is thus a singlet state.

The fully bonded nature of the armchair edge imparts stability to the structure. While direct comparison of (I)/(I)′, (II), and (II) is not possible due to differing molecular formulas, adding one and two hydrogen atoms respectively to vacant sites of (I)/(I)′ and (III) gives molecular formulas of $C_{22}H_{10}$, identical to that of (II), each with two possible binding sites. The energetics of the various structures are shown in Figure 2. The lowest of

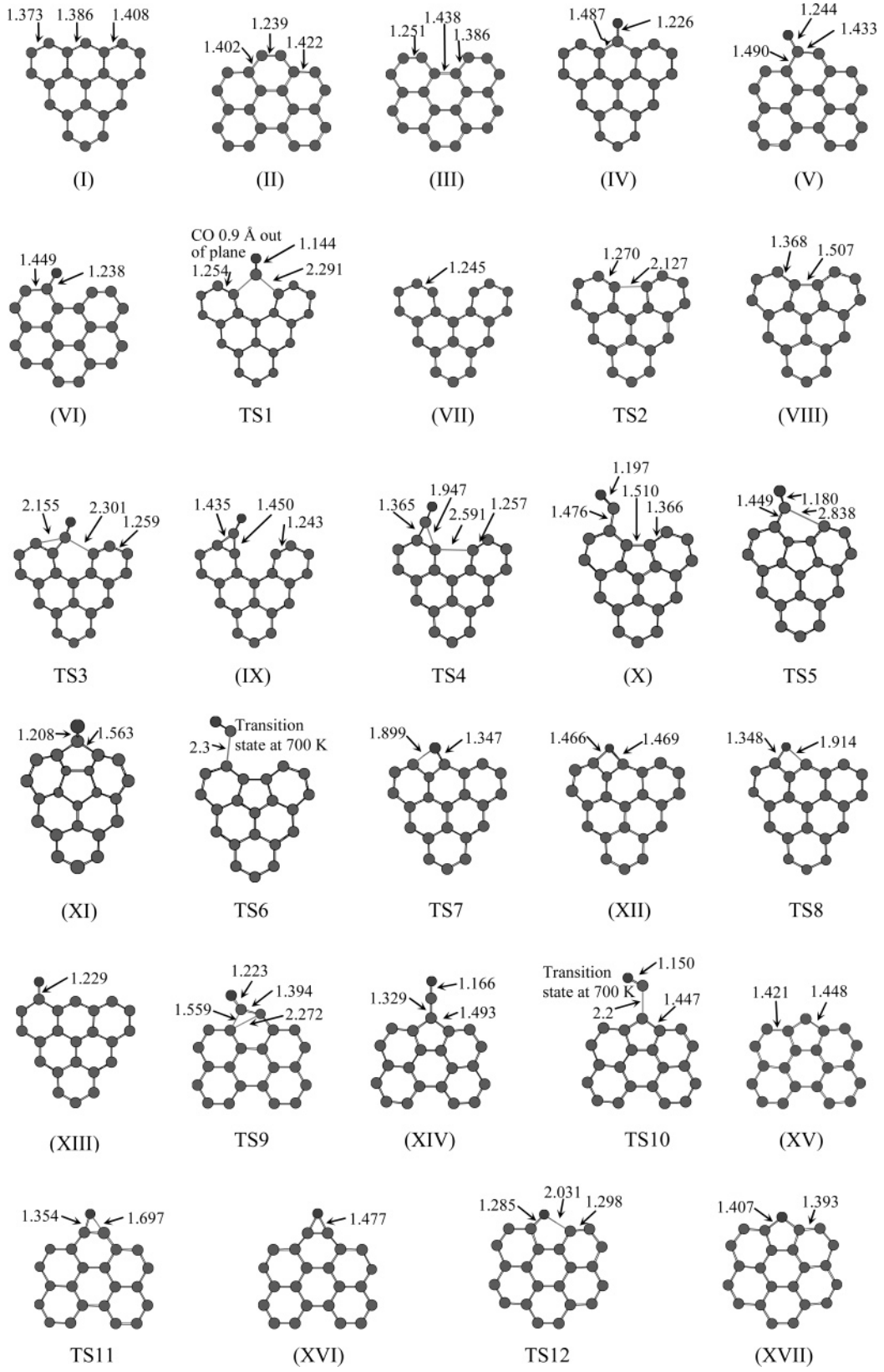


**Figure 3.** Geometrical parameters for stable species and transition states for model chars as in Figure 1. Bond lengths in angstroms.

the $C_{22}H_{10}$ isomers are the singlet benzyne-like isomers based on (II) and (III) + 2H armchair edges. The triplet states of these isomers lie 120−135 kJ mol$^{-1}$ higher in energy, slightly lower than the corresponding value for benzyne at this level of theory.[24] Between 90 and 100 kJ mol$^{-1}$ above the most stable isomers are three species (both singlet and triplet states) with a single hydrogen substitution on each edge aromatic ring, removing the benzyne character from the edge. The lowest isomers on the zigzag edge are the Kekulé based structures of model A′ + H, ∼125 kJ mol$^{-1}$ above the most stable structure on the armchair edge. This is in good agreement with the energy difference between benzyne and the high-spin state of *p*-

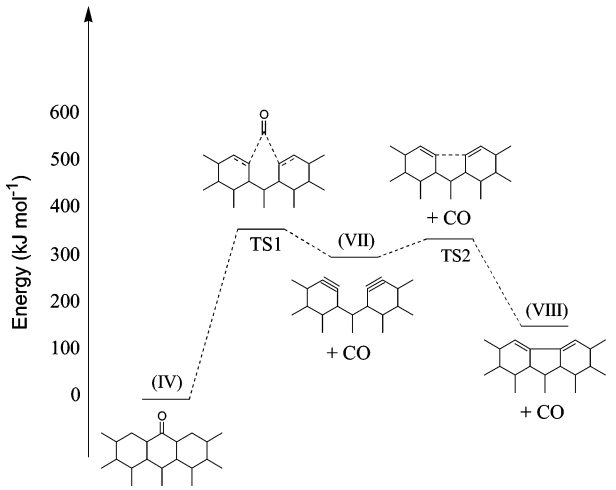


**Figure 4.** Potential energy surface for CO desorption from zigzag surface.

**TABLE 1: Relative Energies of Species on the Zigzag Surface**

| | rel energy (kJ mol$^{-1}$) | | | |
|---|---|---|---|---|
| species | doublet state | quartet state | model A′ ground state | large model A ground state |
| (IV) | 10 | 0 | 0 | 0 |
| TS1 | 354 | 469[a] | | |
| (VII) + CO | 311 | − | 315 | 291 |
| TS2 + CO | 330 | − | | |
| (VIII) + CO | 155 | 148 | 147 | 192 |
| TS3 | 275 | 384 | | |
| (IX) | 174 | 306 | 180,[b] 184[c] | 158 |
| TS4 | 221 | 334 | | |
| (X) | 29 | 31 | 24,[b] 30[c] | 32 |
| TS5 | 56 | − | | |
| TS6 | 151[d] | 144[d] | | |
| (XI) | −69 | 141 | −66 | −23 |
| TS7 | 227 | 213 | 168,[b,e] 173[c,e] | |
| (XII) | 182 | 168 | 107,[b,e] 112[c,e] | 175 |
| TS8 | 227 | 214 | 170,[b,e] 184[c,e] | |
| (XIII) | 12 | 7 | 13,[b] 34[c] | −6 |

[a] Energy estimated from ref 10. [b] Oxide formed with $C_2$. [c] Oxide formed with $C_6$. [d] Geometry obtained using variational TST at 700 K. [e] Species on the doublet surface.

benzyne.[23] The non-Kekulé model A + H chars are ∼210 kJ mol$^{-1}$ higher in energy than on the armchair edge. This indicates that the zigzag edge is thermodynamically more unstable than the armchair edge. The position of the unpaired electrons on the zigzag edge does not significantly affect the energetics.

**Comparison of Ketone on Zigzag and Armchair Surfaces.** Addition of an oxygen atom to either the zigzag or the armchair surface produces a ketone functional group according to the following reaction scheme:

$$(I) + 0.5O_2 \rightarrow (IV) \qquad -407\ (-401)\ \text{kJ mol}^{-1}$$

$$(I)' + 0.5O_2 \rightarrow (IV)' \qquad -340\ \text{kJ mol}^{-1}$$

$$(II) + 0.5O_2 \rightarrow (V) \qquad -194\ (-197)\ \text{kJ mol}^{-1}$$

$$(III) + 0.5O_2 \rightarrow (VI) \qquad -218\ (-194)\ \text{kJ mol}^{-1}$$

The number in parentheses represents the values on the larger model char (Figure 1). (I)′ and (IV)′ correspond to fresh zigzag surface and a ketone group on a model A′ char, respectively. It can be seen that the formation of the ketone on the zigzag surface is 130 (model A′) to 200 (model A) kJ mol$^{-1}$ more exothermic than on the armchair surface. This is the result of the zigzag surface being less thermodynamically stable than the armchair surface.

**TABLE 2: Relative Energies of Species on the Armchair Surface**

| | rel energy (kJ mol$^{-1}$) | | |
|---|---|---|---|
| species | singlet state | triplet state | large models B and C ground state |
| (V) | 16 | 0 | 0 |
| TS9 | 70 | | |
| (XIV) | −140 | 5 | −146 |
| TS10 | 182[a] | 144[a] | |
| (XV) + CO | 203 | 154 | 150 |
| TS11 | 132 | − | |
| (XVI) | 125 | − | 120 |
| (VI) | 6 | 0 | 0 |
| TS12 | 47 | 46 | |
| (XVII) | −72 | −72 | −82 |

[a] Geometry obtained using variational TST at 700 K.

**TABLE 3: Kinetic Parameters for Reactions**

| reaction | forward $A$ factor[a] | forward $E_a$ [b] | reverse $A$ factor[a] | reverse $E_a$ [b] |
|---|---|---|---|---|
| (IV) ↔ (VII) + CO | $1.2 \times 10^{16}$ | 367 | $5.5 \times 10^{11}$ | 53 |
| (VII) ↔ (VIII) | $1.9 \times 10^{12}$ | 19 | $3.1 \times 10^{13}$ | 189 |
| (IV) ↔ (IX) | $2.5 \times 10^{15d}$ | 284 | $8.9 \times 10^{13}$ | 105 |
| (IX) ↔ (X) | $1.4 \times 10^{13}$ | 49 | $5.1 \times 10^{13}$ | 195 |
| (X) ↔ (XI) | $7.1 \times 10^{11}$ | 25 | $1.1 \times 10^{14}$ | 131 |
| (X) ↔ (VIII) + CO | $3.0 \times 10^{14}$ | 117 | $7.0 \times 10^{8} \times T^{1.068\,c}$ | −0.3 |
| (IV) ↔ (XII) | $1.3 \times 10^{13d}$ | 215 | $2.0 \times 10^{13}$ | 48 |
| (XII) ↔ (XIII) | $2.0 \times 10^{13}$ | 49 | $6.5 \times 10^{12}$ | 209 |
| (V) ↔ (XIV) | $6.1 \times 10^{12}$ | 74 | $1.0 \times 10^{13\,d}$ | 214 |
| (XIV) ↔ (XV) + CO | $3.2 \times 10^{15}$ | 296 | $4.7 \times 10^{4} \times T^{2.409\,c}$ | −6.6 |
| (V) ↔ (XVI) | $4.3 \times 10^{12}$ | 135 | $5.4 \times 10^{12\,d}$ | 8.0 |
| (VI) ↔ (XVII) | $2.4 \times 10^{12}$ | 46 | $3.4 \times 10^{13\,d}$ | 123 |

[a] Units: s$^{-1}$ for unimolecular reactions, cm$^3$ mol$^{-1}$ s$^{-1}$ for bimolecular reactions. [b] $E_a$ in kJ mol$^{-1}$. [c] This reaction required a three-parameter fit due to variational TST. [d] This $A$ factor contains a factor of 2 due to symmetry, accounting for reaction in both directions. The $A$ factor should be halved if a single process is to be considered.

The ground state of (IV) is a quartet, with the doublet just 10 kJ mol$^{-1}$ higher in energy. This is in general agreement with the small splitting of 0.4 kJ mol$^{-1}$ calculated by Montoya et al.[9] rather than the 189 kJ mol$^{-1}$ calculated by Frankcombe and Smith.[10] This discrepancy is due to the choice of wave function used to describe a molecule such as (IV). Montoya et al.[9] used an unrestricted wave function to describe both low- and high-spin states of the biradical equivalent of (IV), whereas Frankcombe and Smith[10] used a restricted wave function to describe the low-spin state. This forces the electrons to be paired and thus describes an excited state, possibly related to the allene-type structure noted earlier on the zigzag edge. The structure (IV)′ is just 11 kJ mol$^{-1}$ more stable than (IV), indicating that the structure of the initial model char does not have an effect on the properties of the ketone, as neither (IV) nor (IV)′ can be considered Kekulé structures. The computed C−O and $C_3$−$C_4$ bond lengths are 1.226 and 1.487 Å, respectively, which are similar to the corresponding bond lengths of 1.216 and 1.525 Å in acetone at the same level of theory, indicating that the ketone can be well-described by a C−O double bond and C−C single bonds.

The ground states of both (V) and (VI) are triplet, with low-lying singlet excited states. On the smaller model char, (VI) was found to be ~24 kJ mol$^{-1}$ more stable compared to the larger model char, which is within the errors expected at this level of theory. The computed C−O bonds are ~1.24 Å, with the $C_2-C_3$ bonds in the range of 1.43−1.45 Å and the $C_3-C_4$ bonds ~1.49 Å. This indicates slightly less C−O double bond character and slightly more $C_2-C_3$ double bond character than in the corresponding bonds in the ketone on the zigzag surface.

**Reactions of Ketone on the Zigzag Surface.** *CO Desorption.* Recently, two studies of the desorption behavior of CO from a ketone site on a zigzag edge have appeared,[9,10] with dramatically different findings. Montoya et al.[9] used a model char consisting of five six-membered aromatic rings and performed density functional calculations at the B3LYP level of theory with a spin-unrestricted wave function and the 6−31(*d*) basis set. They found that the singlet and triplet states of the ketone were essentially degenerate and that direct CO loss occurred on the singlet surface via a planar transition state with a barrier of 350 kJ mol$^{-1}$. They used transition-state theory to obtain an *A* factor of 1.81 × 10$^{17}$ s$^{-1}$ and an activation energy of 396 kJ mol$^{-1}$ for this process. They concluded that the product was a closed-ring species and that the overall reaction was 193 kJ mol$^{-1}$ endothermic. Frankcombe and Smith[10] used the same model char, density functional method, and basis set but with a spin-restricted wave function for singlet states. They found that the singlet state of the ketone was ~190 kJ mol$^{-1}$ above the triplet state. They considered both direct CO loss and CO loss via a "surface intermediate". For the direct process, they found that the singlet transition state was nonplanar with a barrier of 177 kJ mol$^{-1}$ above the singlet state of (IV) (366 kJ mol$^{-1}$ above the triplet state of (IV)) and produced an open-ring product (equivalent to (VII)). They found a higher energy triplet transition state leading to CO desorption but did not characterize the product. They computed *A* factors of 9.32 × 10$^{13}$ and 2.19 × 10$^{18}$ s$^{-1}$ and activation energies of 167 and 401 kJ mol$^{-1}$ for the singlet and triplet surfaces, respectively, in disagreement with the earlier study. They found that the final product was a closed-ring species with an endothermicity of 147 kJ mol$^{-1}$ but that this was sensitive to the size of the model char, and they concluded that an open-ring species would be the final product on larger model chars. They also found a lower energy pathway that is best described as a rearrangement reaction, followed by CO desorption and is discussed further in this paper under rearrangement.

The potential energy surface computed in the present study is shown in Figure 4. The ground state of the ketone (IV) is quartet with a low-lying doublet excited state. The direct loss of CO, via TS1, takes place on the doublet surface with a barrier of 354 kJ mol$^{-1}$. TS1 was not found to be planar; rather the departing CO was found to be ~0.9 Å above the plane of the char fragment. This is in agreement with the calculated structure of Frankcombe and Smith rather than the planar structure of Montoya et al., although it should be noted that there is little energetic difference between the computed transition states from Montoya et al.,[9] Frankcombe and Smith,[10] and that presented here. The computed kinetic parameters, however, do not agree with the previous results. In the case of Frankcombe and Smith, this is due to incorrect treatment of the reactant. We expect that if the ground state of the reactant was treated correctly, then our result would be in good agreement with Frankcombe and Smith. In the case of Montoya et al., we believe that the difference is due to the planarity of their transition state. The breaking C−C bonds are shortened in the nonplanar transition state, decreasing the *A* factor and reducing the calculated activation energy for CO loss from 397 to 367 kJ mol$^{-1}$.

To understand why the energy of the low-spin transition state is significantly lower than the high-spin transition state, the nature of the transition state must be understood. As the C−C bonds were broken, it was noted that the distance between $C_3$ and $C_5$ increases.[9] However, the $C_2-C_3$ and $C_5-C_6$ bonds simultaneously decrease to a value of 1.25 Å, equivalent to a benzyne triple bond. Thus, the formation of two "armchair" edges on either side of the departing CO stabilizes the transition state for the lowest spin state, causing the doublet state to be significantly lower in energy than the quartet state. The formation of the triple bonds effectively pairs the electrons, allowing the closed-shell wave function[10] to describe the low-spin transition state adequately. If an additional functional group were to bind to either $C_2$ or $C_6$, a triple bond could not be formed and the stabilization would be reduced, increasing the barrier for CO loss.[25]

The low-spin transition state TS1 initially produces (VII), an open-ring product identified by Frankcombe and Smith, rather than the closed-ring species (VIII) identified by Montoya et al. However, as the barrier to ring closure (TS2) was just 18 kJ mol$^{-1}$ above (VII), it is unlikely that the open-ring species would be stabilized as an intermediate.

Attention must be given to the final product of the reaction, the five-membered ring (VIII). Our computations place this structure 148 kJ mol$^{-1}$ above (IV), in agreement with 147 kJ mol$^{-1}$ found by Frankcombe and Smith and ~45 kJ mol$^{-1}$ lower in energy than found by Montoya et al.[9] Unlike the discrepancies described earlier in this section, the source of this error can be identified as the failure to use redundant internal coordinates in the study by Montoya et al., resulting in an incorrect (i.e. not a true local minimum) product geometry.

Finally, the effect of changing of the model char is considered. As can be seen from Table 1, the energetics of the lowest state for each of the stable molecules is, within the expected error of the method, insensitive to the choice of model A or model A′. This indicates that for oxides which break any possible Kekulé structure (e.g. those with double bonds to the carbon edge), either model is suitable for computing energetics and kinetic parameters. The energetics are also found to be insensitive to increasing char size, with the exception of (VIII). The closed, five-membered ring structure is computed to be ~50 kJ mol$^{-1}$ less stable on the larger model char, in agreement with the suggestion by Frankcombe and Smith[10] that increasing the char size destabilized (VIII). Although nonplanar, it has similar $C_3-C_5$ bond length to the structure identified by Montoya et al.[9] on the smaller char and exists at a similar energy. No structure corresponding exactly to (VIII) on the smaller char could be identified on the larger char. However, the closed-ring structure is still more stable than the open-ring structure and would be expected to be the final product of the direct CO desorption, rather than the open-ring structure as suggested by Frankcombe and Smith. Given the good agreement between the smaller and larger model chars for (IV) and (VII), it is expected that the rate constant for direct CO desorption would not change with char size.

*Rearrangement.* As proposed by Frankcombe and Smith,[10] an alternate path to CO loss can occur via rearrangement of the ketone as shown in Figure 5. On the singlet surface, they found that the migration reaction to form the surface complex occurs with an activation energy of 93 kJ mol$^{-1}$, with CO loss from the surface complex having an activation energy of 149 kJ mol$^{-1}$. On the triplet surface, they found a three-step process:

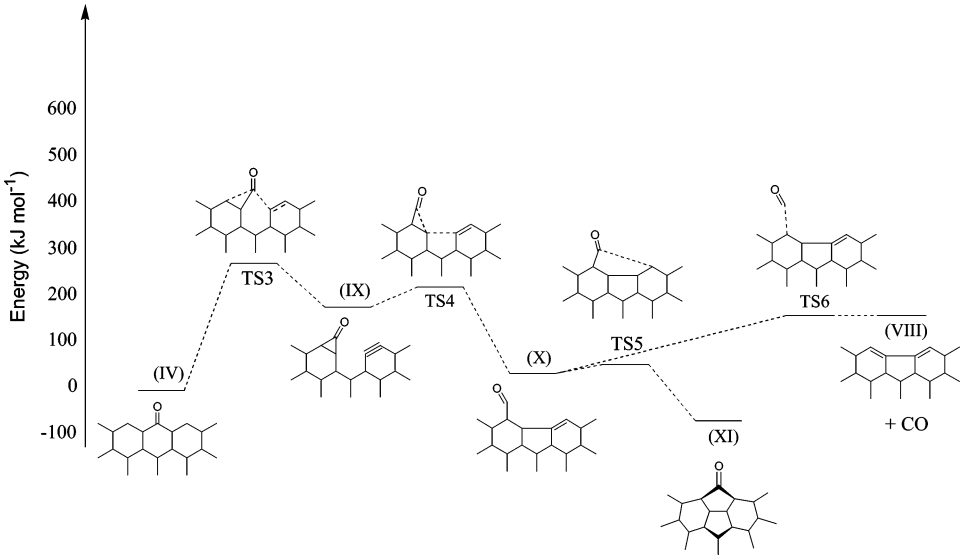


**Figure 5.** Potential energy surface for oxide rearrangement on zigzag surface. ▲ indicates distortions above the plane.

formation of surface complex ($E_a$ = 335 kJ mol$^{-1}$) and then ring closure ($E_a$ = 29 kJ mol$^{-1}$) followed by gasification ($E_a$ = 121 kJ mol$^{-1}$).

The potential energy surface computed in the present study for the rearrangement reaction is shown in Figure 5. Initially, the $C_4-O$ carbonyl group migrates via TS 3 to form a three-membered ring (IX). This reaction occurs on the low-spin surface, due to the triple bond formed between $C_5$ and $C_6$, with a barrier of 275 kJ mol$^{-1}$ and an endothermicity of 174 kJ mol$^{-1}$, in good agreement with 288 and 178 kJ mol$^{-1}$ found earlier.[10] This barrier is ∼80 kJ mol$^{-1}$ lower than the barrier for direct CO loss, and this process, if an adjacent site were free (i.e. $C_2$ or $C_6$ was available for formation of a three-membered ring), would be expected to be much more important than direct CO loss. The rate constant reported in Table 3 for the process (IV) → (IX) contains a symmetry factor of 2 and describes migration to both $C_2$ and $C_6$. Cleavage of the $C_3-C_4$ bond and concomitant formation of the $C_3-C_5$ bond occurs readily via TS4 to produce a stable intermediate (X), with degenerate doublet and quartet states. This is in disagreement with Frankcombe and Smith,[10] who found that gasification would occur directly from the low-spin state of (IX). However, their result is a consequence of their choice of a spin-restricted wave function, which is unable to describe the low-spin state of (X).

As the doublet state of (X) is slightly lower in energy than the quartet state, some bonding interaction between the unpaired electrons must occur in the doublet state. This interaction is between $C_1$ and $C_6$, and a low-barrier pathway via TS5 on the doublet surface produces (XI), the most stable oxide identified on the zigzag surface, 69 kJ mol$^{-1}$ lower in energy than (IV). This oxide, which is quite nonplanar and resembles a structure found in small fullerenes, would be expected to be less stable in a multilayer char system. Due to the extreme nonplanarity of (XI) and TS5, it was assumed that there was a substantial barrier to forming their mirror images, and this was reflected in the treatment of the kinetics by including a factor of 2 in the partition functions.

Although (XI) has a plane of symmetry, loss of CO from (XI) does not occur through a symmetric transition state; the two C−C bonds are broken sequentially with (X) as an intermediate. The *A* factor reported in Table 3 for the process (XI) → (X) does not contain a symmetry factor of 2; it describes only the cleavage of the $C_4-C_6$ bond, and not the symmetrically equivalent cleavage of the $C_2-C_4$ bond, which produces a mirror image of (X). Desorption of CO from (X) to produce (VIII) occurs via TS6 with an activation energy of 117 kJ mol$^{-1}$, which was located variationally because no saddle point could be located. The high-spin state of this reaction was described in the previous study[10] and is in good agreement with the energetics described here. Due to the small barrier to form the more stable (XI), it is unlikely that (X) would be stabilized on the smaller model char; thus, it is not expected that the CO desorption process (X) → (VIII) + CO would be experimentally observed with an activation energy of 117 kJ mol$^{-1}$. Instead, the process (XI) → (VIII) + CO would be observed, with an activation energy similar to the endothermicity of the reaction, i.e., ∼215 kJ mol$^{-1}$.

The relative energetics of (IX) and (X) are calculated to be insensitive to increasing the size of the model char, indicating that the rate constants for their formation would be unchanged. Oxide (XI) is ∼40 kJ mol$^{-1}$ less stable on the larger oxide, although still the most stable oxide species on the surface. Since the closed-ring structure (VIII) is ∼45 kJ mol$^{-1}$ less stable on the larger model char, loss of CO from (XI) would appear to proceed with an essentially unchanged activation energy. On the larger model char, however, it is more likely that (X) could be stabilized, especially if TS5 was also ∼40 kJ mol$^{-1}$ higher in energy. In this case, an extra desorption process would appear at ∼160 kJ mol$^{-1}$, causing a broadening of the activation energy distribution. No difference was found between model chars A and A′ for this reaction.

*Migration.* In addition to undergoing CO loss, a ketone group can also migrate along the zigzag edge, via a four-membered ring (XII) as shown in Figure 6. The barrier to this reaction is 213 kJ mol$^{-1}$ (TS7), substantially lower in energy than either direct CO loss or rearrangement to (X). The *A* factor reported in Table 3 for the process (IV) → (XII) includes migration to both $C_2$ and $C_6$ and would need to be halved to describe migration to a single site. This is why the forward *A* factor for the process is twice that for the apparently equivalent process (XIII) → (XII). The intermediate (XII) has C−O bonds of 1.47 Å, 0.2 Å longer than the ketone (IV); has a curved rather than planar structure; and is 162 kJ mol$^{-1}$ above the intermediate. Reaction through TS8 to produce (XIII) completes a single step of surface migration. In the case of an infinite edge, TS8 would be equivalent to TS7; similarly (XIII) would be equivalent to (IV). Even if $C_2$ is at the end of a zigzag edge (as in model A and reported here), the computed energetics are quite similar,

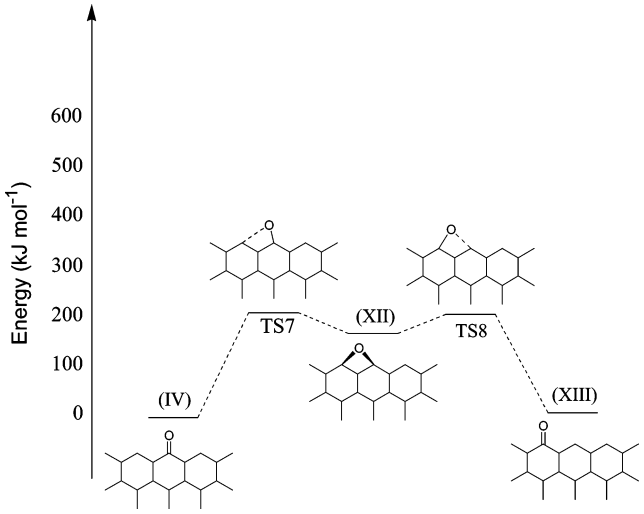


**Figure 6.** Potential energy surface for oxide migration on zigzag surface. ▲ indicates distortions above the plane.

with TS8 and (XIII) 227 and 7 kJ mol$^{-1}$ above (IV), respectively. Due to the relatively low barrier of TS8 above (XII), it is unlikely that the four-membered ring would be stabilized as an intermediate. The energetics of the species involved in the migration reaction are insensitive to increasing the size of the model char.

Oxides (IV) and (XIII) exist at similar energies for models A and A′ as neither are Kekulé structures, but this is not true for the intermediates (XII)/(XII)′. On the model char A′, Kekulé structures are possible for the doublet states of (XII)′, and the equivalent structures are ∼60 kJ mol$^{-1}$ lower in energy than (XII) on the model A char. The transition states for migration TS7′ and TS8′ were computed to be ∼40 kJ mol$^{-1}$ lower on model char A′ than TS7 and TS8 on model char A, indicating that the migration process would be considerably faster on a Kekulé based char structure. The lowering of the barrier for migration by ∼40 kJ mol$^{-1}$ is attributable to a difference in the bonding patterns, i.e., partial Kekulé structure, rather than to error associated with the quantum chemical method.

**Reactions of Ketone on the Armchair Surface.** *Rearrangement.* While oxygen may exist on the armchair surface as a ketone, two low-barrier pathways to form more stable oxide structures exist, resulting in a short lifetime for a ketone. The first low-barrier reaction requires no adjacent aromatic ring and is discussed here as a rearrangement reaction and shown in Figure 7; the second low barrier pathway requires an adjacent aromatic ring and is part of the surface oxide migration pathway discussed later.

The ketone on the armchair surface (V), with its biradical character, can undergo rearrangement to form a five-membered ring with an attached ketene group (XIV) as shown in Figure 7. The transition state for this reaction (TS9) involves cleaving the $C_1-C_2$ bond and simultaneously forming a bond between $C_1$ and $C_3$. This transition state occurs on the singlet surface and is just 70 kJ mol$^{-1}$ above the ground state of (V). The ketene formed, (XIV), also has a singlet ground state, is 140 kJ mol$^{-1}$ below (V), and is the most stable oxide identified on the armchair surface.

*CO Desorption.* Attempts to locate a transition state for the direct loss of CO from (V) were unsuccessful, consistently collapsing onto TS9. In any event, since the barrier to formation of (XIV) is low, it is likely that any CO loss would occur from (XIV) rather than (V). Loss of CO from (XIV) involves cleaving the $C_2-C_3$ bond to produce (XV), with a triplet ground state.

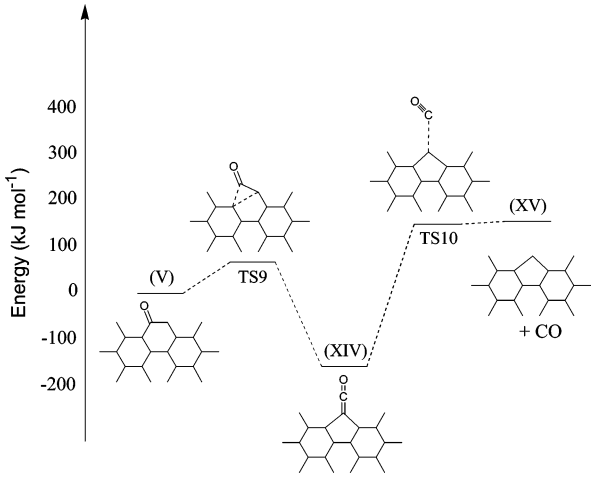


**Figure 7.** Potential energy surface for oxide rearrangement and CO desorption from armchair surface.

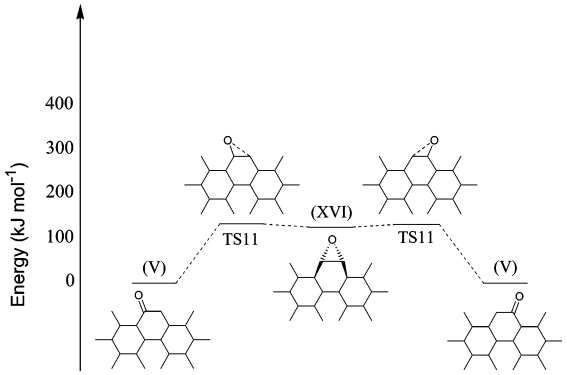


**Figure 8.** Potential energy surface for oxide migration within a single ring on armchair surface. ▲ and △ indicate distortions above and below the plane, respectively.

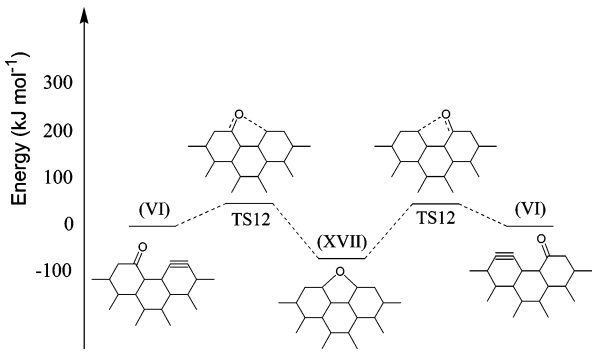


**Figure 9.** Potential energy surface for oxide migration between two rings on armchair surface.

This reaction was found to have no barrier in addition to the endothermicity of reaction (294 kJ mol$^{-1}$), requiring the use of variational transition-state theory in order to calculate the rate constant. The reported geometry of TS10 is the geometry applicable to the temperature range 700−1700 K.

*Migration.* Migration of the oxygen atom along the armchair edge can occur either across one aromatic ring (Figure 8) or from one aromatic ring to the next (Figure 9). Migration across one ring occurs via a singlet epoxide intermediate (XVI), 125 kJ mol$^{-1}$ above the ketone (V). As the barrier to re-forming a ketone (TS11) is just 7 kJ mol$^{-1}$, it is unlikely that the epoxide (XVI) would be stabilized. The *A* factor for the reaction (XVI) → (V) includes a symmetry factor of 2 to allow for migration to both $C_2$ and $C_3$.

Migration of the oxygen atom from one aromatic ring to the next occurs via a furan intermediate (XVII), 72 kJ mol$^{-1}$ below the starting ketone (VI). With a barrier of just 46 kJ mol$^{-1}$ (TS12), this reaction will proceed rapidly and it is likely that (XVII) will be stabilized as an intermediate and will be a major reaction product (along with (XIV)) below CO desorption temperatures of ketone on the armchair surface. The *A* factor for the reaction (XVII) → (VI) includes a symmetry factor of 2. Loss of CO from (XVII) is expected to occur via the ketone and ketene structures.

The energies for all species on the armchair surface considered here were found to be insensitive to increasing the size of the model char, within the error of the computational method.

**Relating the Computed Potential Energy Surface to Experimental Observables.** *Surface Oxides.* The potential energy surfaces obtained in this study reveal a number of isomers of ketone that could easily be formed under combustion conditions. Indeed, on the armchair surface, if $C_3$ is vacant,[11] the rearrangement reaction to form the ketene (XIV) will occur at room temperature ($k \sim 1$ s$^{-1}$ at 300 K) and if an adjacent ring is present with a vacant site, the partial migration reaction to form a furan (XVII) will occur rapidly at room temperature ($k \sim 2 \times 10^4$ s$^{-1}$ at 300 K). If a ketone group on the zigzag surface was exposed to higher temperatures, the carbonyl group (X) and the fullerene group (XI) would be observed, along with some gasification. Such a discussion ignores the role of the formation process: if the ketone is formed by an exothermic process, it may not be stabilized, rather it may readily undergo rearrangement and migration reactions. It is unlikely that the migration intermediate on the zigzag surface (XII) would be stabilized, even if the char had an underlying Kekulé structure.

*Desorption Behavior.* Experimentally, the activation energy for desorption has a broad profile, and the reactions considered here can account for this type of behavior. On the zigzag surface, direct desorption of CO occurs with an activation energy of ~370 kJ mol$^{-1}$; this will be higher if functional groups on either (or both) $C_2$ or $C_6$ prohibit the stabilization of the transition state.[25] CO desorption via a three-ring intermediate (IX) would be observed with an activation energy of ~280 kJ mol$^{-1}$; this would be higher if either $C_2$ or $C_6$ were not vacant, and this process would not occur if neither $C_2$ nor $C_6$ were free. Reaction via (IX) can also result in the stabilization of (XI), and also (X): desorption of CO from these species would have activation energies of ~210 and ~160 kJ mol$^{-1}$, respectively. On the armchair surface, loss of CO from the stable ketene (XIV) has an activation energy of ~300 kJ mol$^{-1}$, and loss of CO from the stable furan (XVII) would appear with an activation energy of ~230 kJ mol$^{-1}$. It is clear that char surface (zigzag/armchair) and oxide structure affect not only the breadth of the activation energy profile but also surface coverage. Defects in the char structure can also have an effect, especially on structures involving five-membered rings.[11]

**Relating the Computed Potential Energy Surface To Model Development.** The pathways presented here include desorption pathways, as well as rearrangement and surface migration pathways. It is clear that these occur on much shorter time scales than the desorption pathways. This has implications for scrambling effects: although a particular oxide structure may form at a particular vacant site, the oxide will neither necessarily remain in that particular form nor desorb from that particular site.

Although increasing the size of the model char has an effect on the thermochemistry of some species, it appears that the kinetics of most processes studied here will be insensitive to increasing the char size. This indicates that model chars containing six aromatic rings are suitable for describing the kinetic behavior of a single graphite sheet as well as more realistic char fragments. While different behavior and properties were expected for the zigzag and armchair surfaces, previous work on a range of model chars with zigzag surfaces[21] had not noted any differences between non-Kekulé and Kekulé structures. While chemisorption reactions, and to a lesser extent migration reactions, on the different forms of the zigzag edge will need to be treated separately, this work has shown that rearrangement and desorption of ketones can be modeled using either form of the zigzag edge and consideration can be given to other factors such as symmetry when choosing appropriate model chars for these reactions. Since interconversion between the two forms will occur as carbon atoms are removed due to gasification, it is important to include both forms in a model, not just the more stable Kekulé form.

## 4. Conclusions

This work presents a systematic study of the reactions of ketones on both the zigzag and armchair surfaces of a model carbon char. The zigzag and armchair edges have been characterized, with the armchair edge being the most stable due to its benzyne-like structure, followed by the Kekulé zigzag edge, with the non-Kekulé zigzag edge highest in energy. The difference between the two zigzag edges is significant for chemisorption reactions, as well as oxides bound with only single bonds. A number of desorption, rearrangement, and surface migration reactions that are energetically accessible under normal reaction conditions have been characterized. The rearrangement and surface migration reactions occur on much shorter time scales than the desorption reactions, and consideration should be given to this when developing mechanisms for carbon gasification. The experimentally observed broad activation energy profile for desorption can be partially explained by the range of reactions presented here.

The importance of using unrestricted wave functions to describe biradical systems and redundant internal coordinates has been shown for these systems.

**Acknowledgment.** The work has been funded by the Australian Research Council and by the University of Sydney through the HB and FM Gritton Bequest. The computations were carried out at the Australian Centre for Advanced Computing and Communication (AC3) at Australian Technology Park, Sydney, and the Australian Partnership for Advanced Computing (APAC) at the Australian National University, Canberra.

## References and Notes

(1) Haynes, B. S. *Combust. Flame* **2001**, *126*, 1421−1432.
(2) Ma, M. C.; Brown, T. C.; Haynes, B. S. *Surf. Sci.* **1993**, *297*, 312−326.
(3) Zhu, Z.; Lu, G. Q. (M.); Finnerty J.; Yang, R. T. *Carbon* **2003**, *41*, 635−658.
(4) Zhu, Z. H.; Finnerty, J.; Lu, G. Q.; Yang, R. T. *Energy Fuels* **2002**, *16*, 1359−1368.
(5) Zhu, Z. H.; Finnerty, J.; Lu, G. Q.; Wilson, M. A.; Yang, R. T. *Energy Fuels* **2002**, *16*, 847−854.
(6) Montoya, A.; Mondràgon, F.; Troung, T. N. *Fuel Process. Technol.* **2002**, *77*−*78*, 125−130.
(7) Montoya, A.; Mondràgon, F.; Troung, T. N. *Carbon* **2003**, *41*, 29−39.
(8) Espinal, J. F.; Montoya, A.; Mondràgon, F.; Troung, T. N. *J. Phys. Chem. B* **2004**, *108*, 1003−1008.
(9) Montoya, A.; Mondràgon, F.; Truong, T. N. *J. Phys. Chem. A* **2002**, *106*, 4236−4239.
(10) Frankcombe, T. J.; Smith, S. C. *Carbon* **2004**, *42*, 2921−2928.

(11) Sendt, K.; Haynes, B. S. *Proc. Combust. Inst.*, in press.
(12) Allinson, G.; Bushby, R. J.; Paillaud, J.-L.; Thornton-Pett, M. *J. Chem. Soc., Perkin Trans.* **1995**, 385−390.
(13) Chen, N.; Yang, R. T. *Carbon* **1998**, *36*, 1061−1070.
(14) Perry. S. T.; Hambly, E. M.; Fletcher, T. H.; Solum, J.; Pugmire, R. J. *Proc. Combust. Inst.* **2000**, *28*, 2313−2319.
(15) Thomson, K. T.; Gubbins, K. E. *Langmuir* **2000**, *16*, 5761−5773.
(16) Montoya, A.; Truong, T. N.; Sarofim, A. F. *J. Phys. Chem. A* **2000**, *104*, 6108−6110.
(17) Gräfenstein, J.; Kraka, E.; Filatov, M.; Cremer, D. *Int. J. Mol. Sci.* **2002**, *3*, 360−394.
(18) Fogarasi, G.; Zhou, X.; Taylor, P.; Pulay, P. *J. Am. Chem. Soc.* **1992**, *114*, 8191−8201.
(19) High Performance Computational Chemistry Group. *NWChem, A Computational Package for Parallel Computers, Version 4.0.1*; Pacific Northwest National Laboratory: Richland, WA2001, 2001.
(20) Frisch, M. J.; et al. *Gaussian 98*, Revision A; Gaussian, Inc.: Pittsburgh, PA, 1998.
(21) Chen, S. G.; Yang, R. T.; Kapteijn, F.; Moulijn, J. A. *Ind. Eng. Chem. Res.* **1993**, *32*, 2835−2840.
(22) Stein, S. E.; Brown, R. L. *J. Am. Chem. Soc.* **1987**, *109*, 3721−3729.
(23) Hou, S.; Shen, Z.; Zhao, X.; Xue, Z. *Chem. Phys. Lett.* **2003**, *373*, 308−313.
(24) de Visser, S. P.; Filatov, M.; Schreiner, P. R.; Shaik, S. *Eur. J. Org. Chem.* **2003**, 4199−4204.
(25) Sendt K.; Haynes, B. S. Manuscript in preparation.